Regulation of Calcium Channels and Exocytosis in Mouse Adrenal Chromaffin Cells by Prostaglandin EP3 Receptors

Mark L. Jewell, Richard M. Breyer, and Kevin P. M. Currie

Departments of Anesthesiology (K.P.M.C.), Biochemistry (R.M.B.), Medicine (R.M.B.), and Pharmacology (M.L.J., R.M.B., K.P.M.C.), Vanderbilt University School of Medicine, Nashville, Tennessee

ABSTRACT

Prostaglandin (PG) E_2 controls numerous physiological functions through a family of cognate G protein-coupled receptors (EP1–EP4). Targeting specific EP receptors might be therapeutically useful and reduce side effects associated with nonsteroidal anti-inflammatory drugs and selective cyclooxygenase-2 inhibitors that block prostanoid synthesis. Systemic immune challenge and inflammatory cytokines have been shown to increase expression of the synthetic enzymes for PGE_2 in the adrenal gland. Catecholamines and other hormones, released from adrenal chromaffin cells in response to Ca^{2+} influx through voltage-gated Ca^{2+} channels, play central roles in homeostatic function and the coordinated stress response. However, long-term elevation of circulating catecholamines contributes to the pathogenesis of hypertension and heart failure. Here, we investigated the EP receptor(s) and cellular mechanisms by which PGE_2 might modulate chromaffin cell function. PGE_2 did not alter resting intracellular $[Ca^{2+}]$ or the peak amplitude of nicotinic acetylcholine receptor currents, but it did inhibit Ca_V2 voltage-gated Ca^{2+} channel currents (I_{Ca}). This inhibition was voltage-dependent and mediated by pertussis toxin-sensitive G proteins, consistent with a direct $G\beta\gamma$ subunit-mediated mechanism common to other $G_{i/o}$-coupled receptors. mRNA for all four EP receptors was detected, but using selective pharmacological tools and EP receptor knockout mice, we demonstrated that EP3 receptors mediate the inhibition of I_{Ca}. Finally, changes in membrane capacitance showed that Ca^{2+}-dependent exocytosis was reduced in parallel with I_{Ca}. To our knowledge, this is the first study of EP receptor signaling in mouse chromaffin cells and identifies a molecular mechanism for paracrine regulation of neuroendocrine function by PGE_2.

Introduction

Catecholamines and other hormones released from adrenal chromaffin cells help maintain normal homeostatic function and play central roles in the coordinated response to acute stressors, for example, during "fight-or-flight" sympathetic activation. Elevation of circulating catecholamines is closely correlated with hypertension and is a hallmark of chronic heart failure. Indeed, specifically targeting the adrenal gland to inhibit catecholamine outflow in vivo improved cardiac function in rat models of heart failure, suggesting adrenal hormone release as a potential therapeutic target (Lymperopoulos et al., 2008). In situ, acetylcholine (ACh) released from splanchnic nerve fibers activates nicotinic ACh receptors on the chromaffin cell, causing membrane depolarization, opening of voltage-gated calcium channels, and influx of calcium that subsequently triggers exocytosis (Boarder et al., 1987). Thus, as with neurons and other excitable cells, voltage-gated calcium channels play pivotal roles in chromaffin cell function. The cells also express a variety of G protein-coupled receptors (GPCRs) that orchestrate complex regulation of stimulus-secretion coupling. For example, chromaffin cells express autoreceptors for ATP (P2Y receptors), catecholamines (α-adrenergic), and enkephalin (μ-opioid receptors) that couple to $G_{i/o}$-type G proteins and mediate autocrine/paracrine inhibition of catecholamine release through inhibition of voltage-gated calcium channels (Albillos et al., 1996; Currie and Fox, 1996; Harkins and Fox, 2000; Powell et al., 2000; Ulate et al., 2000) and other downstream targets (Chen et al., 2005; Yoon et al., 2008).

In this study, we investigated the effects of prostaglandin (PG) E_2 on chromaffin cells. PGE_2 is produced in a variety of cell types through metabolism of arachidonic acid by cyclooxygen-

ABBREVIATIONS: ACh, acetylcholine; DG-041, (2E)-3-[l-[(2,4-dichlorophenyl)methyl]-5-fluoro-3-methyl-1H-indol-7-yl]-N-[(4,5-dichloro-2-thienyl)sulfonyl]-2-propenamide; COX, cyclooxygenase; RT-PCR, reverse transcriptase-polymerase chain reaction; GAPDH, glyceraldehyde-3-phosphate dehydrogenase; nAChR, nicotinic acetylcholine receptor; PGE_2, prostaglandin E_2; GPCR, G protein-coupled receptor; Cm, membrane capacitance.

ase (COX-1 or COX-2) and prostaglandin E synthases. It acts in an autocrine/paracrine manner, primarily through binding to a family of cognate GPCRs (EP1–EP4 receptors) (Breyer et al., 2001) to control a variety physiological functions, including protection of the gastric mucosa, renal function, inflammation, pain, blood pressure, and secretion of hormones and neurotransmitters. Nonsteroidal anti-inflammatory drugs such as aspirin and selective COX-2 inhibitors reduce the production of PGE_2 but also disrupt synthesis of other prostanoids and can cause serious side effects. One strategy to reduce these unwanted side effects is to identify specific cellular functions of EP receptors and develop EP receptor subtype-selective drugs. For example, characterization of EP receptor signaling in smooth muscle suggests that EP1 receptors could be targeted for antihypertensive treatment, and an EP3 receptor antagonist (2*E*)-3-[l-[(2,4-dichlorophenyl)methyl]-5-fluoro-3-methyl-1*H*-indol-7-yl]-*N*-[(4,5-dichloro-2-thienyl)sulfonyl]-2-propenamide (DG-041) is under investigation for treatment of atherothrombosis (Guan et al., 2007; Heptinstall et al., 2008).

EP1 and EP3 receptors are expressed in the adrenal medulla (Breyer et al., 1993; Namba et al., 1993; Shibuya et al., 1999; Engström et al., 2008) along with the synthetic enzymes for PGE_2 (Ichitani et al., 2001; Engström et al., 2008). Moreover, systemic immune challenge or circulating cytokines rapidly recruit dendritic cells and macrophages to the adrenal gland and increase the expression of COX-2 and PGE synthase and presumably local PGE_2 production (Engström et al., 2008). Thus, the components are in place for local modulation of chromaffin cells by PGE_2, but previous studies present confusing and contradictory findings: PGE_2 has been reported to increase (Marley et al., 1988; Yamada et al., 1988; Yokohama et al., 1988; Karaplis et al., 1989) or decrease (Karaplis et al., 1989) adrenal catecholamine release, elevate intracellular calcium levels (Mochizuki-Oda et al., 1991; Shibuya et al., 1999), or inhibit voltage-gated calcium channels (Currie et al., 2000). In sympathetic neurons, which are closely related to chromaffin cells, PGE_2 can modulate nicotinic ACh receptors (Tan et al., 1998; Du and Role, 2001) and voltage-gated calcium channels (Ikeda, 1992). Thus, PGE_2 may alter calcium signaling and exocytosis in chromaffin cells by multiple pathways and potentially through multiple EP receptors.

The goal of this study was to define the receptors and mechanisms by which PGE_2 modulates calcium signaling in adrenal chromaffin cells using a combination of pharmacological tools and EP receptor knockout mice. We show that PGE_2 did not alter the peak amplitude of nicotinic ACh receptor currents or resting intracellular $[Ca^{2+}]$ but potently inhibited Ca_V2 voltage-gated calcium channel currents (I_{Ca}) ($EC_{50} = 5.5$ nM). Although mRNA for all four EP receptor subtypes is expressed in the mouse adrenal gland, our data unequivocally show that EP3 receptors mediate this inhibition of I_{Ca}. PGE_2 also decreased the change in membrane capacitance in response to membrane depolarization/calcium entry, suggesting that the number of secretory vesicles undergoing exocytosis was reduced. To our knowledge, this is the first study of EP receptor signaling in mouse chromaffin cells and identifies a cellular/molecular mechanism for paracrine regulation of neuroendocrine function by PGE_2.

Materials and Methods

Cell Preparation and Culture. Male mice (6–12 weeks old), wild-type, EP3 receptor knockout (Y. Zhang, C. E. Swan, K. I. Boyd, A. Bian, A. Shintani, D. Lee, D. W. Threadgill, R. C. Harris, R. Zent, and R. M. Breyer, manuscript in preparation), or EP1 receptor knockouts (Guan et al., 2007), all on C57BL/6 background, were euthanized using carbon dioxide followed by cervical dislocation. Adrenal glands were quickly harvested and placed in ice-cold magnesium-free Locke's solution containing 153 mM NaCl, 6 mM KCl, 2 mM $NaH_2PO_4 \cdot 7H_2O$, 1 mM $NaH_2PO_4 \cdot H_2O$, 10 mM glucose, and mM 10 HEPES. The glands were trimmed of fat, and the cortex was dissected from the medullae. The medullae were incubated for 15 min at 37°C in a papain digestion solution (2.5 mg/ml papain; Genlantis, San Diego, CA) followed by another 10-min incubation at 37°C in collagenase P (3 U/ml; Roche Diagnostics, Indianapolis, IN). Tissues were washed two times with Locke's and transferred to growth medium consisting of Dulbecco's modified Eagle's medium/F-12/GlutaMAX (Invitrogen, Carlsbad, CA) supplemented with HyClone-defined fetal bovine serum (10%) (Thermo Fisher Scientific, Waltham, MA) and penicillin (100 U/ml)/streptomycin (100 μg/ml) (Sigma-Aldrich, St. Louis, MO). Tissues were then triturated with a 2 ml of fire-polished glass pipette coated in growth medium and allowed to settle. The cell containing supernatant was removed and plated on glass coverslips thinly coated in growth factor-reduced Matrigel (BD Biosciences Discovery Labware, Bedford, MA). Cells were allowed to settle and adhere to the coverslips for 2 h before 2 ml of growth medium was added to the coverslips. Cells were maintained at 37°C in a humidified, 5% CO_2 atmosphere and used 1 to 3 days after isolation. Each cell preparation was from a single mouse. All experimental studies were approved by the Institutional Animal Care and Use Committee of Vanderbilt University Medical Center.

Electrophysiology. Electrodes were pulled from borosilicate glass capillary tubes (World Precision Instruments, Sarasota, FL), coated with dental wax (Electron Microscopy Sciences, Hatfield, PA) and fire-polished to a final resistance of 1.8 to 3 MΩ when filled with a CsCl-based internal solution. Cells were voltage-clamped in the whole-cell configuration using an Axopatch 200B amplifier, Digidata1400A interface, and pClamp10 software (Molecular Devices, Sunnyvale, CA). Analog data were filtered at 2 kHz and digitized at 20 μs/point (50 kHz). Data were analyzed using pClamp10, OriginPro software (OriginLab Corp, Northampton MA), and Prism version 5 (GraphPad Software Inc., San Diego, CA). For perforated whole-cell recording configuration, the pipette tip was filled with amphotericin-free solution and then backfilled with solution that contained ~0.5 mg/ml amphotericin B (Calbiochem, San Diego, CA). After forming a cell-attached seal, series resistance was monitored to assess the progress of perforation. Typically, series resistance <10 to 15 MΩ was achieved within 5 to 15 min, and cells that did not show good perforation within this time frame were discarded. I_{Ca} was activated by brief 20- to 100-ms step depolarizations to a predetermined peak (10–30 mV) from a holding potential of -80 mV. Data were subjected to linear capacitance and leak subtraction using standard pulse/number (P/N) protocols. When determining the inhibition of I_{Ca} produced by PGE_2 (100 nM), cells in which the current amplitude decreased <10% were designated as "nonresponders" and are reported as such under *Results*. Only "responders" (i.e., >10% current decrease) were included when calculating the mean percentage of inhibition. The presence of both responders and nonresponders was consistently observed in multiple cell preparations, but we did not investigate any other possible differences between the two sets of cells in this study. To calculate an EC_{50} for inhibition of I_{Ca} by PGE_2, data were fit with a Boltzmann function of the form $Y = Y_{max}/(1 + 10^{(\log EC_{50} - X)})$; where Y is the percentage of inhibition of I_{Ca}, and X is the concentration of PGE_2. The Hill slope was assumed to be 1, and the curve fit with the least-squares method in Prism 5 software. Goodness of fit was indicated by $R^2 = 0.97$.

Nicotinic ACh receptor currents were activated by bath perfusion for 45 s with 30 to 100 μM carbachol. This enabled multiple reproducible responses to be obtained from the same cell. The delay in current activation (Fig. 3A) was due to the "dead space" in the perfusion system. The amplitude of the sustained inward current activated by carbachol was determined by calculating the mean current amplitude over a 5-s period starting 30 s after carbachol application. The mean current amplitude over this 5-s period was determined for each cell, and then data were pooled. The current amplitude was also calculated (mean over a 5-s period) at the end of the drug application to determine the extent to which the response declined.

Changes in membrane capacitance (ΔCm) were monitored in the perforated whole-cell recording configuration using a HEKA EPC10 amplifier in combination with PatchMaster data acquisition software (HEKA, Lambrecht/Pfalz, Germany). The software lock-in module was used to implement the "sine + d.c." approach for estimating Cm. A sine wave (1-kHz, 20-mV peak to peak) was imposed on the holding potential of -80 mV, and the assumed reversal potential was set to 0 mV. The software simultaneously calculated membrane conductance (Gs), and any cells that showed simultaneous changes in Cm and Gs were discarded. Cells were stimulated by two-step depolarizations (to +10 mV, 100-ms duration) separated by 100 ms. The stimulus was repeated every 3 min. Membrane capacitance was averaged over a 50-ms period before the stimulus (baseline) and again 50 ms after the end of the stimulus to calculate ΔCm. After two control responses, cells were exposed to 100 nM PGE$_2$ during the third response. The second control response was typically of equal or greater magnitude than the first, and if this was not the case, the cell was discarded because of concern about "rundown." For data analysis, cells were divided into those that responded to PGE$_2$ with decrease in I$_{Ca}$ amplitude >10% (group 1) and those in which I$_{Ca}$ was not inhibited (group 2) (see *Results* for more discussion). Data are reported as mean $\pm$ S.E.M., and statistical significance was determined using paired or independent Student's t test as appropriate.

[Ca^{2+}]$_i$ Measurements. Free cytosolic Ca^{2+} concentration ([Ca^{2+}]$_i$) was measured in cells loaded with the fluorescent Ca^{2+} indicator Fura-2 (Invitrogen, Carlsbad, CA). Cells were washed twice with HEPES-buffered Hanks' balanced salt solution and incubated for 30 to 45 min with 3 μM Fura-2 acetoxymethyl ester at 37°C. Cells were then washed in Fura-free solution for 30 to 60 min before recording. For recording, the coverslip with the cells attached was transferred to a recording chamber and mounted on the stage of a Nikon TE2000 fluorescence microscope (Nikon, Tokyo, Japan). The recording chamber had a volume of ~300 to 400 μl and was continually perfused with fresh solution from gravity-fed reservoirs at a flow rate of ~4 ml/min. An InCyt IM2 fluorescence imaging system (Intracellular Imaging Inc., Cincinnati, OH) was used to monitor [Ca^{2+}]$_i$. Cells were alternately excited at wavelengths of 340 and 380 nm and emission at 510 nm detected using a PixelFly digital camera as detailed previously (Dzhura et al., 2006). Ratios were collected every 2 s throughout the experiment and converted to [Ca^{2+}]$_i$ using an in vitro calibration curve, generated by adding 15.8 μM Fura-2 pentapotassium salt to solutions from a calibration kit containing 1 mM MgCl$_2$ and known concentrations of Ca^{2+} (0–1350 nM) (Invitrogen). One or two cells in the field of view were selected in each experiment and after a 2-min baseline were exposed to 1 μM PGE$_2$ for 3 min and subsequently to a 50 mM KCl-containing solution (by replacing an equimolar amount of NaCl in our standard extracellular solution; see below). This was done as a positive control for the assay to ensure the cells were loaded with Fura-2 and responded to calcium elevations. It also served as a means to identify any nonexcitable (i.e., nonchromaffin) cells because these typically fail to respond to KCl. Cells that had an unstable baseline or failed to respond robustly to KCl (>300 nM elevation) were excluded from analysis. Data analysis was performed using OriginPro software (OriginLab Corp).

RT-PCR. Total RNA was prepared from mouse adrenal and kidney tissue using QIAGEN RNeasy Mini Kit (QIAGEN, Valencia, CA). cDNA was synthesized from total RNA with ABI High-Capacity Reverse Transcriptase kit (Applied Biosystems, Foster City, CA) and amplified using specific primers: EP1, 5′-TTAACCTGAGCCTAGCGGATG-3′ (sense primer, nucleotides 311–331), 5′-CGCTGAGCGTATTGCACACTA −3′ (antisense primer, nucleotides 956–976); EP2, 5′-CCTGGGACATGGT-GCTTTAT-3′ (sense primer, nucleotides 1404–1423), 5′-GGTGGCCTA-AGTATGGCAAA-3′ (antisense primer, nucleotides 1797–1816); EP3c, 5′-CGCCGTCTCGCAGTC-3′ (sense primer, nucleotides 849–863); EP3$\alpha\beta$, 5′-TGTGTCGTCTTGCCCCCG-3′ (antisense primer, nucleotides 1362–1379); EP3γ, 5′-TGTGGCTTCATTCCTTGCCCA-3′ (antisense primer, nucleotides 1572–1592); EP4, 5′-GGTCATCTTACTCATCGC-CACCTCTC-3′ (sense primer, nucleotides 1027–1052, 5′-TCCCACTA-ACCTCATCCACCAACAG-3 (antisense primer, nucleotides 1562–1586); and GAPDH, 5′-GGCATTGCTCTCAATGACAA-3′ (sense primer, nucleotides 942–961), 5′-TGTGAGGGAGATGCTCAGTG-3′ (antisense primer, nucleotides 1122–1141).

Drugs and Solutions. Cells were perfused at a rate of ~4 ml/min with external solution consisting of 136 mM NaCl, 2 mM KCl, 1 mM MgCl · 6H$_2$O, 10 mM glucose, 10 mM HEPES, and 10 mM CaCl · 2H$_2$O, pH 7.3, with osmolarity of ~305. All drugs were diluted ($\geq$1000×) and perfused in this extracellular solution unless otherwise noted. For whole-cell recordings, electrodes were filled with internal solution containing 110 mM CsCl, 10 mM EGTA, 20 mM HEPES, 4 mM MgCl$_2$, 0.35 mM GTP, 4 mM ATP, and 14 mM creatine phosphate, pH 7.3, with osmolarity of ~305. The free calcium concentration in this solution is estimated to be very low (<1 nM) (http://maxchelator.stanford.edu). For perforated whole-cell recording, electrode tips were filled with internal solution containing 145 mM cesium glutamate, 10 mM HEPES, 10 mM NaCl, and 1 mM tetraethylammonium chloride, pH 7.3, with osmolarity of 309, and backfilled with internal solution containing amphotericin B (Calbiochem) at a final concentration of 0.53 mM, prepared from a 100× stock solution in dimethyl sulfoxide every 2 h. PGE$_2$ (Cayman Chemical Company, Ann Arbor, MI) and Sulprostone (Sigma-Aldrich) were prepared as 10 mM stock solutions in ethanol and dimethyl sulfoxide, respectively, and frozen until the day of use. DG-041 was synthesized in the Vanderbilt Institute of Chemical Biology Chemical Synthesis Core. Pertussis toxin (Calbiochem) was prepared as a 100 μg/μl stock in water and applied 24 h before experiment in cell culture medium at 300 ng/μl. Carbachol (Calbiochem) and tetrodotoxin (Alomone Labs, Jerusalem, Israel) were prepared in sterile water as 100 and 1 mM stocks, respectively, and diluted on the day of use. Nitrendipine (ICN Biomedicals Inc., Aurora, OH) was prepared as a 10 mM stock solution in ethanol and diluted to 10 μM in external solution. Stock solutions of ω-conotoxin GVIA (100 μM) (Alomone Labs) and ω-agatoxin IVA (10 μM) (Bachem Biosciences, King of Prussia, PA) were prepared in standard extracellular solution and diluted to final working concentrations of 1.5 μM and 400 nM, respectively, on the day of use.

Results

PGE$_2$ Inhibits I$_{Ca}$ in Mouse Adrenal Chromaffin Cells. Given the pivotal roles of voltage-gated calcium channels in stimulus-secretion coupling and many other cellular functions, we initially tested whether PGE$_2$ inhibited the calcium channel currents (I$_{Ca}$) in mouse chromaffin cells. The cells were voltage-clamped at -80 mV and stimulated with a 20-ms step depolarization to evoke I$_{Ca}$ every 10 s (Fig. 1A). Application of 100 nM PGE$_2$ produced a significant and reversible inhibition of peak I$_{Ca}$ amplitude (Fig. 1A) in approximately 76% of cells tested under similar experimental conditions (conventional whole-cell recording, $n = 37$ of 49 cells, $n = 9$ mice). The inhibition of I$_{Ca}$ was concentration dependent (Fig. 1B) and the data fit well with a Boltzmann func-

tion that yielded a maximal inhibition of 40% and an EC_{50} of 5.5 nM consistent with the low nanomolar affinities reported for PGE_2 binding to EP receptors (Breyer et al., 2001).

The Inhibition of I_{Ca} by PGE_2 Is Voltage-Dependent and Mediated by Pertussis Toxin-Sensitive G Proteins. GPCRs inhibit I_{Ca} by several different mechanisms, but perhaps the most widespread and best understood pathway is mediated by direct binding of G protein $\beta\gamma$ subunits to P/Q-type ($Ca_V2.1$) and N-type ($Ca_V2.2$) channels (Currie, 2010a). Although there are exceptions, in most cases, this pathway involves GPCRs that couple to pertussis toxin-sensitive $G_{i/o}$-type G proteins. We and others have shown previously that P2Y purinergic receptors and μ-opioid receptors use this pathway to produce autocrine/paracrine inhibition of I_{Ca} in chromaffin cells (Albillos et al., 1996; Currie and Fox, 1996; Powell et al., 2000). To determine whether PGE_2 acts through a $G_{i/o}$-coupled GPCR, we incubated isolated mouse chromaffin cells with pertussis toxin (300 ng/ml) for ~24-h before whole-cell recording. Control cells were from the same cell preparations and were recorded on the same days as the pertussis toxin-treated cells. As shown in Fig. 2A, the inhibition of I_{Ca} produced by PGE_2 was virtually abolished in

pertussis toxin-treated cells ($2 \pm 2.6\%$, $n = 6$, compared with $31 \pm 7.1\%$, $n = 7$, in control cells; $p < 0.002$). As a positive control, we also used the P2Y receptor agonist ATP (100 μM), because this is known to inhibit I_{Ca} via pertussis toxin-sensitive G proteins in chromaffin cells (Currie and Fox, 1996). The inhibition produced by ATP was also significantly reduced ($29 \pm 8.5\%$, $n = 7$ in control cells compared with $7 \pm 5.4\%$, $n = 6$, in pertussis toxin-treated cells; $p < 0.05$). These data confirmed that PGE_2 acts though a $G_{i/o}$-coupled GPCR to inhibit I_{Ca}.

A defining biophysical signature of direct $G\beta\gamma$-mediated inhibition of N- and P/Q-type channels is reversal by a strongly depolarizing voltage step. This reversal is believed to reflect transient dissociation of $G\beta\gamma$ from the channel at the depolarized membrane potential (Currie, 2010a). Therefore, we used a prepulse facilitation protocol to determine whether PGE_2 used
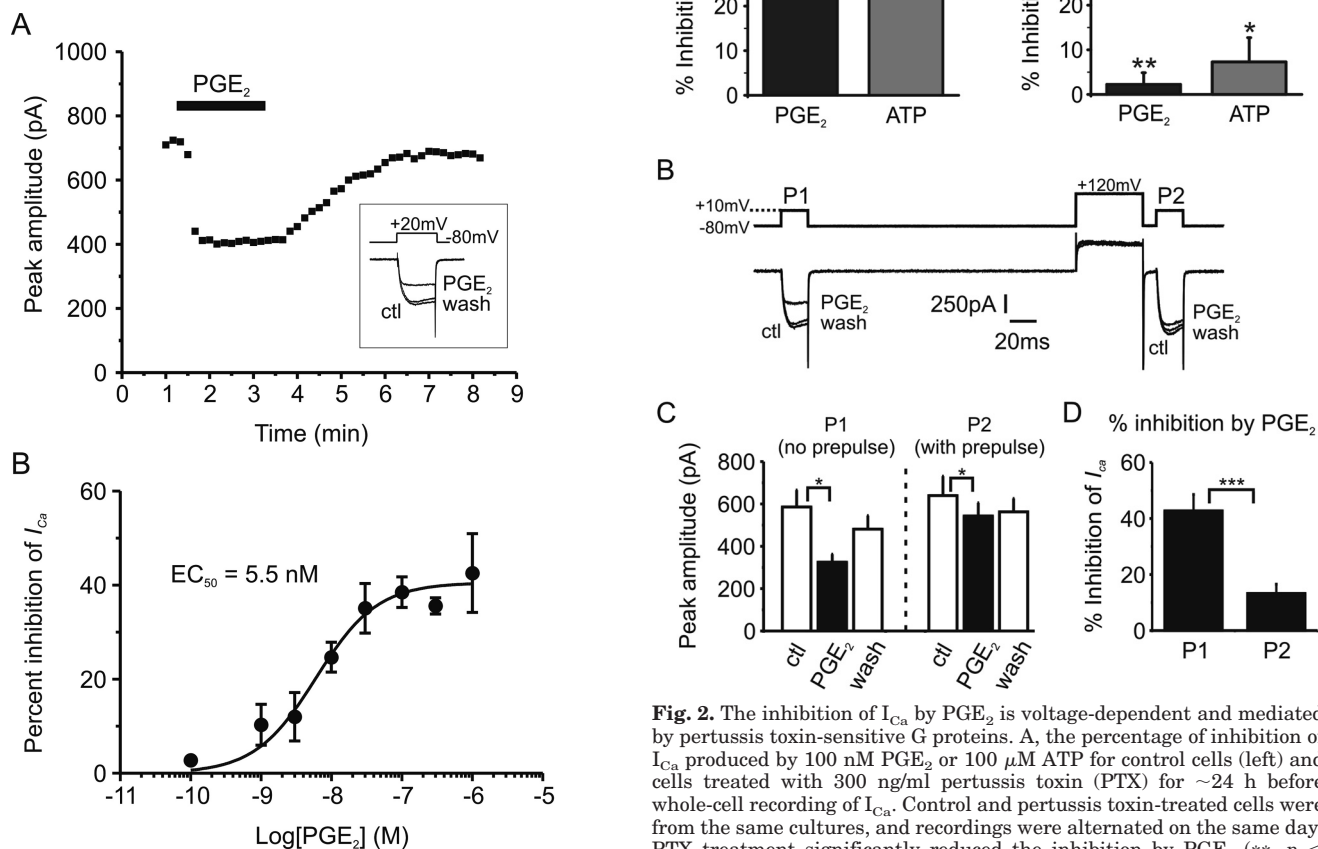

Fig. 1. PGE_2 inhibits I_{Ca} in mouse adrenal chromaffin cells. A, peak amplitude of I_{Ca} is plotted against time in a representative cell. The cell was voltage-clamped in the whole-cell configuration and stimulated with a 20-ms step depolarization from −80 to +20 mV every 10 s. Application of PGE_2 (100 nM) (indicated by horizontal bar) produced robust, reversible inhibition of I_{Ca}. Inset, the voltage command (top) and three representative current traces before (ctl), during (PGE_2), and after washout of PGE (wash). B, Log_{10} concentration-response curve plotting percentage of inhibition of I_{Ca} to varying concentrations of PGE_2. Each cell was exposed to three increasing concentrations of PGE_2, with 10 nM being common to all experiments ($n = 4$–16 cells). The indicated fit was to a Boltzmann function with a Hill slope of 1 (see *Materials and Methods*) and yielded an EC_{50} of 5.5 nM.

Fig. 2. The inhibition of I_{Ca} by PGE_2 is voltage-dependent and mediated by pertussis toxin-sensitive G proteins. A, the percentage of inhibition of I_{Ca} produced by 100 nM PGE_2 or 100 μM ATP for control cells (left) and cells treated with 300 ng/ml pertussis toxin (PTX) for ~24 h before whole-cell recording of I_{Ca}. Control and pertussis toxin-treated cells were from the same cultures, and recordings were alternated on the same day. PTX treatment significantly reduced the inhibition by PGE_2 (**, $p < 0.002$) and ATP (*, $p < 0.05$). B, the inhibition of I_{Ca} by PGE_2 was voltage-dependent. Top, the voltage command for the prepulse facilitation protocol. Cells were stimulated by two identical test pulses (P1 and P2, 20-ms step to +10 mV, separated by 300 ms), but the second pulse (P2) was preceded by a 50-ms step to +120 mV. Three representative currents are superimposed (bottom trace), showing I_{Ca} before (ctl), during application of 100 nM PGE_2 (PGE_2), and after washout (wash). The prepulse to +120 mV reversed most of the inhibition of I_{Ca} produced by PGE_2. C, mean data from six experiments like that shown in B. Bar chart summarizes the mean peak amplitude of I_{Ca} during the first pulse (P1, no prepulse) and the second pulse (P2, with prepulse) (*, $p < 0.05$; $n = 6$). D, the percentage inhibition by PGE_2 of I_{Ca} elicited by P1 (without a prepulse) and P2 (with a prepulse) (***, $p < 0.001$; $n = 6$).

this mechanism to inhibit I_{Ca} in mouse chromaffin cells. Figure 2B illustrates a representative voltage command (top) and current trace (bottom). The cell was stimulated by two identical test pulses (P1 and P2), the second of which was preceded by a 50-ms step to +120 mV. PGE_2 significantly reduced the amplitude of I_{Ca} during both P1 and P2 (Fig. 2C), but the prepulse (immediately preceding P2) significantly reduced this inhibition from $43 \pm 6\%$ during P1 to $13 \pm 3\%$ during P2 ($n = 6$; $p < 0.001$) (Fig. 2D). Thus, the inhibition of I_{Ca} produced by PGE_2 was largely voltage-dependent, although there was also a voltage-independent component to the inhibition (the residual inhibition seen during P2) consistent with what has been reported previously for P2Y and opioid receptors.

Voltage-dependent inhibition of I_{Ca} by other GPCRs preferentially targets the Ca_V2 family of calcium channels, in particular P/Q-type ($Ca_V2.1$) and N-type ($Ca_V2.2$) channels (Currie, 2010a). Mouse chromaffin cells are known to express Ca_V2 channels (P/Q-, N-, and R-type channels) and members of the Ca_V1 family (L-type channels) (García et al., 2006). Consistent with previous reports, we found that nitrendipine, a dihydropyridine antagonist of L-type channels, blocked $41 \pm 5\%$ ($n = 7$) of the whole-cell current. We did not systematically dissect the channel types comprising the non–L-type current, but previous reports indicate the majority is carried by N- and P/Q-type channels, with 10 to 20% accounted for by R-type and perhaps T-type channels (García et al., 2006). After block of N-type ($Ca_V2.2$) and P/Q-type ($Ca_V2.1$) channels by preincubation with ω-conotoxin GVIA (1.5 μM) and ω-agatoxin IVA (400 nM), respectively, the inhibition by PGE_2 was dramatically reduced ($7 \pm 1\%$, $n = 6$; $p < 0.05$) confirming that N- and P/Q-type channels are the main target for this pathway.

Short-Term Application of PGE_2 Did Not Alter Peak Nicotinic Acetylcholine Receptor Currents. In situ, chromaffin cells are directly innervated by cholinergic splanchnic nerve fibers. Activation of nicotinic acetylcholine receptors (nAChRs) on the chromaffin cells causes membrane depolarization, activation of voltage-gated calcium channels, and influx of calcium that triggers exocytosis. It has been reported that PGE_2 modulates nicotinic acetylcholine receptors in sympathetic neurons (Tan et al., 1998; Du and Role, 2001), although we are not aware of any similar studies in chromaffin cells. However, it has been shown that inhibition of nAChRs in chromaffin cells can reduce cytosolic calcium elevations and catecholamine release elicited by cholinergic stimuli (Dzhura et al., 2006). Thus, PGE_2 could indirectly alter calcium channels and calcium signaling in chromaffin cells by modulating nAChR.

To test this possibility, cells were voltage-clamped at a holding potential of −80 mV in the perforated whole-cell recording configuration, and the bath was continuously perfused with fresh extracellular recording solution. Nicotinic ACh receptor currents were evoked by application of 100 μM carbachol for 45 s (Fig. 3A). Under these conditions, the inward current was primarily due to the relatively nondesensitizing nACh receptors found in chromaffin cells. After washout of carbachol, the cells were allowed to recover for 6 min before exposure to 100 nM PGE_2 and a second application of 100 μM carbachol (in the continued presence of PGE_2) (Fig. 3A). Short-term application of PGE_2 had no effect on the mean peak inward current evoked by carbachol (351 ± 65 pA in the presence of PGE_2 compared with 352 ± 63 pA before

application of PGE_2; $n = 8$) (Fig. 3B). The inward current response did decay slightly during continued application of carbachol ($9 \pm 2\%$ in control conditions), and this was significantly increased in the presence of PGE_2 ($21 \pm 3\%$; $p < 0.01$).

Short-Term Application of PGE_2 Did Not Elevate Basal Intracellular Calcium Concentration. Previous reports indicated that relatively high concentrations of PGE_2 ranging from 200 nM to 1 μM can directly elevate intracellular calcium concentration ($[Ca^{2+}]_i$) either by activating a Ca^{2+} influx pathway or by releasing Ca^{2+} from intracellular stores (Mochizuki-Oda et al., 1991; Shibuya et al., 1999). However, in the experiments investigating the effects of PGE_2 on nAChR currents, PGE_2 did not alter the holding current of chromaffin cells voltage-clamped at −80 mV (Fig. 3A), suggesting that PGE_2 did not activate an inward calcium current. We also used Fura-2 imaging to determine whether PGE_2 could elevate resting $[Ca^{2+}]_i$ in individual mouse chromaffin cells. Our data showed that a short-term (3-min) application of 1 μM PGE_2 had no effect on $[Ca^{2+}]_i$ (82 ± 15 nM before and 85 ± 16 nM during application of PGE_2; $n = 9$ cells from seven independent experiments) (Fig. 3C).

mRNA for All Four EP Receptor Subtypes Was Detected in Mouse Adrenal Tissue. The data presented above demonstrate that PGE_2 acts through a $G_{i/o}$-coupled GPCR to inhibit I_{Ca} in mouse chromaffin cells. Of the four known receptors for PGE_2, termed EP1 to EP4, only EP3 typically couples to $G_{i/o}$-type G proteins, although it has been reported that EP1 receptors might also couple to $G_{i/o}$ at least in some cell types (Ji et al., 2010). Both EP3 and EP1 receptors have been reported previously in the adrenal medulla (Breyer et al., 1993; Namba et al., 1993; Engström et al., 2008).
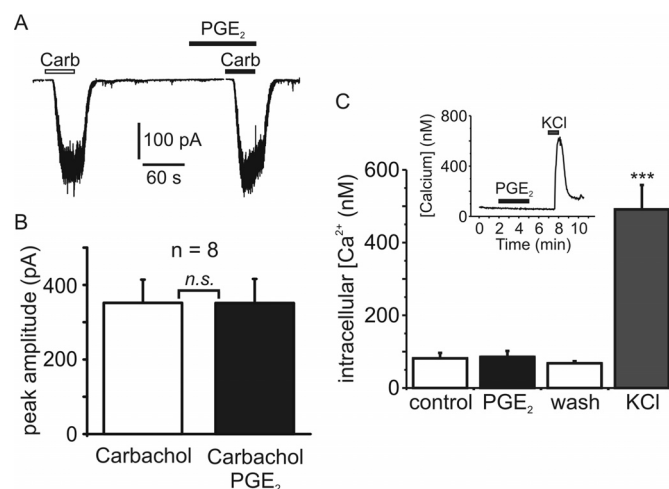

Fig. 3. PGE_2 does not alter peak nicotinic acetylcholine receptor currents or resting $[Ca^{2+}]_i$ in mouse chromaffin cells. A, representative recording of nAChR currents evoked by two applications of carbachol (100 μM) in the absence (left) or presence (right) of 100 nM PGE_2. Drug application is indicated by the horizontal bars. Cells were voltage-clamped at −80 mV in the perforated whole-cell recording configuration. B, bar chart showing that PGE_2 had no effect on the mean amplitude of the nAChR currents evoked by carbachol ($n = 8$ cells). C, ratiometric imaging of Fura-2-loaded chromaffin cells. Inset, a representative recording from a single cell plotting estimated $[Ca^{2+}]_i$ against time (sampling rate, 0.5 Hz). The cell was exposed to 1 μM PGE_2 for 3 min and then to 50 mM KCl to depolarize the membrane and elicit Ca^{2+} entry through voltage-gated Ca^{2+} channels (positive control). The main chart shows mean $[Ca^{2+}]_i$ before (control), during (PGE_2), and after washout (wash) of 1 μM PGE_2 and the response to 50 mM KCl ($n = 9$ cells from seven independent experiments).

To determine which EP receptors were expressed in the mouse adrenal gland we used RT-PCR. The adrenal gland was isolated as described under *Materials and Methods,* and kidney tissue, which expresses all four EP receptor subtypes, was isolated in parallel as a positive control. The adrenal cortex was dissected from the gland leaving the adrenal medulla for RNA isolation; however, small traces of cortex were probably present. Three known splice variants of the EP3 receptor are found in mice: EP3α, EP3β, and EP3γ (Irie et al., 1993; Breyer et al., 2001). The C-terminal tails of these splice variants are different, and the variants can exhibit different downstream signaling pathways and agonist-dependent desensitization in heterologous expression systems. We detected mRNA for all three EP3 receptor splice variants in the mouse adrenal tissue (Fig. 4A). We also detected mRNA for the EP1, EP2, and EP4 receptors (Fig. 4B). GAPDH was used as an internal standard and amplified in all tissues (data not shown).

Pharmacological Evidence that EP3 Receptors Mediate the Inhibition of I_{Ca} by PGE_2. We showed that the inhibition of I_{Ca} was abolished in pertussis toxin-treated cells (Fig. 2A), so is mediated by $G_{i/o}$-coupled GPCRs. Although we detected mRNA for all four EP receptor subtypes in the mouse adrenal gland (Fig. 4), generally, only EP3 receptors couple to $G_{i/o}$ (Breyer et al., 2001). Therefore, we used EP receptor subtype-selective agonists and antagonists to investigate the involvement of EP3 receptors. First, we used the selective EP1/EP3 receptor agonist sulprostone (Fig. 5, A and B). In these experiments, we used perforated whole-cell recordings to maintain endogenous calcium buffering of the chromaffin cells. The inhibition produced by 100 nM PGE_2 ($43 \pm 6\%$, $n = 15$) was similar to that in conventional whole-cell recording. Sulprostone (100 nM) significantly reduced the amplitude of I_{Ca} in six of seven cells by $41 \pm 9\%$ ($n = 6$), and this was not significantly different from the inhibition produced by 100 nM PGE_2 under the same recording conditions ($p = 0.89$).

It has been reported that DG-041 is a selective, noncompetitive antagonist of EP3 receptors (Heptinstall et al., 2008). Cells were stimulated every 10 s with a 20-ms step depolarization to evoke I_{Ca}. DG-041 (30 nM) was applied to the cells for ~2 min before the application of PGE_2 (100 nM). DG-041

alone had little effect on I_{Ca} but completely blocked the inhibition produced by PGE_2 ($2.0 \pm 2.2\%$, $n = 9$; Fig. 5, C and D). Subsequent applications of PGE_2 after several minutes of washout of DG-041 also produced no inhibitory effect, suggesting that DG-041 is functionally irreversible over the time course of our experiments. As a control, we used ATP (100 μM) to activate P2Y receptors in the presence of DG-041. ATP inhibited I_{Ca} by $26 \pm 4.7\%$ ($n = 4$) (Fig. 5D), similar to the inhibition produced by ATP in the absence of DG-041 ($29 \pm 8.5\%$; Fig. 2B). This suggests that DG-041 selectively blocked PGE_2, and the downstream signaling pathways responsible for voltage-dependent inhibition of I_{Ca} were intact.

The Inhibition of I_{Ca} Produced by PGE_2 Was Abolished in Cells Isolated from EP3 Receptor Knockout Mice. The pharmacological data presented above strongly implicated EP3 receptors in the inhibition of I_{Ca} by PGE_2. However, it was still possible that other receptors could play a role. For example, DG-041 is reported to be a selective noncompetitive antagonist of EP3 receptors but off-target effects of the compound have not been widely studied. Therefore, to unequivocally identify the receptor subtype involved, we isolated chromaffin cells from EP3 receptor knockout mice [EP3($-/-$) mice]. As shown in Fig. 6, the inhibition of I_{Ca} by PGE_2 was abolished in cells isolated from EP3($-/-$) mice. In the same cells, 100 μM ATP significantly reduced the amplitude of I_{Ca} by $33 \pm 7\%$ ($n = 6$, $p < 0.05$), indicating

Fig. 5. Pharmacological evidence that EP3 receptors mediate the inhibition of I_{Ca} by PGE_2. A, the selective EP1/EP3 receptor agonist sulprostone inhibits I_{Ca}. Representative voltage command (top) and I_{Ca} (bottom) recorded in presence and absence of sulprostone (100 nM) obtained in the perforated whole-cell recording configuration. B, bar chart illustrating the mean percentage of inhibition of I_{Ca} produced by PGE_2 (100 nM) or sulprostone (100 nM). The inhibition produced by the two agonists was not significantly different. C and D, DG-041, a selective EP3 receptor antagonist, blocked the inhibition of I_{Ca} produced by PGE_2. C, experimental time course in a representative cell plotting peak amplitude of I_{Ca} against time. DG-041 (30 nM) was applied ~2 min before PGE_2 (100 nM) and completely blocked the inhibition of I_{Ca} but had no effect on the inhibition produced by the P2Y receptor agonist ATP (100 μM). D, bar chart summarizing the percentage of inhibition of I_{Ca} by the application of 30 nM DG-041 alone (DG) and in the presence of either 100 nM PGE_2 (DG + PGE_2; $n = 9$) or 100 μM ATP (DG + ATP; $n = 4$). DG-041 prevented the inhibition produced by PGE_2 but not that produced by ATP.
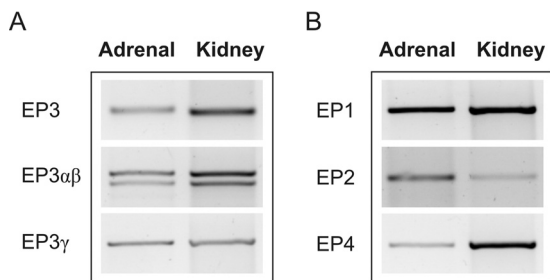
Fig. 4. EP receptor mRNA expressed in mouse adrenal tissue. A, RT-PCR was used to detect expression of the EP3 receptor in mouse adrenal tissue (left) and kidney tissue (right) that was isolated in parallel as a positive control. Top, primers common to all splice variants of the EP3 receptor were used. Bottom, primers selective for the splice variants were used. The forward primers for EP3α and EP3β are identical so the fragments run in the same lane (middle): the top band corresponds with the expected amplicon size of EP3α and the bottom band EP3β . B, in addition to EP3, EP1 (top), EP2 (middle), and EP4 (bottom) mRNA were amplified. All samples from A and B expressed the internal standard GAPDH (data not shown). Data shown are representative of three replicate experiments on tissue from three different mice.
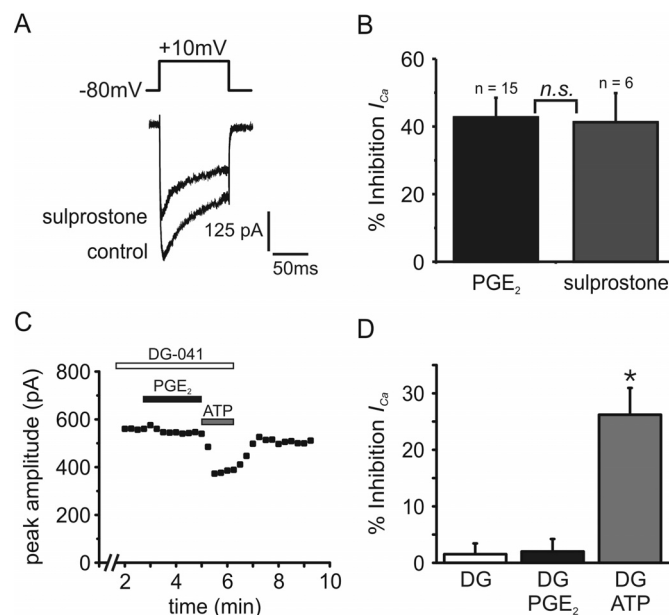
that the effect of the knockout was selective for PGE_2 and did not perturb G protein-mediated inhibition of I_{Ca} by other receptors. Likewise, in perforated whole-cell recording, PGE_2 did not inhibit I_{Ca} in cells isolated from EP3(−/−) mice (1 ± 4% inhibition; $n = 6$).

As a complementary approach, we tested the ability of sulprostone (an EP1/EP3 selective agonist) to inhibit I_{Ca} in cells isolated from EP1 receptor knockout mice. Under these conditions, any effect of sulprostone can be attributed to EP3 receptor signaling because the EP1 receptors are absent. Sulprostone inhibited I_{Ca} in these EP1(−/−) chromaffin cells by 47 ± 12% ($n = 4$), an effect that was not significantly different from that seen in chromaffin cells from wild-type mice (41 ± 9%; $n = 6$). Taken together, our data using pharmacological approaches and knockout mice demonstrate the inhibition of I_{Ca} by PGE_2 is mediated solely by EP3 receptors.
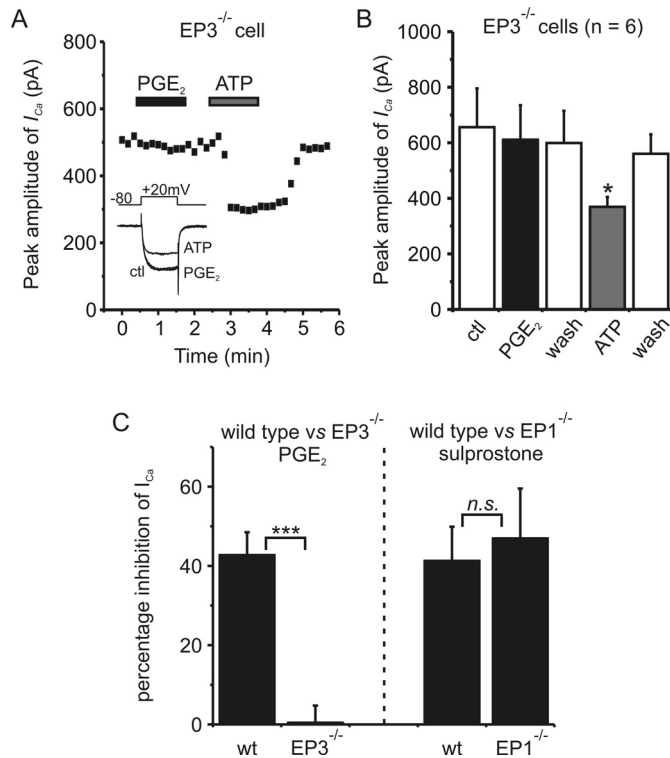
Effects of PGE_2 on Ca^{2+}-Dependent Exocytosis. Ca^{2+} influx through voltage-gated calcium channels is the primary trigger for fusion of large dense-core vesicles with the plasma membrane (i.e., Ca^{2+}-dependent exocytosis). Inhibition of I_{Ca} is believed to an important mechanism that controls neuro-secretion, and a number of GPCRs inhibit I_{Ca} and exocytosis in parallel in adrenal chromaffin cells (García et al., 2006; Currie, 2010b). Membrane capacitance precisely reflects the surface area of a cell and transiently increases when secre-tory vesicles fuse with the plasma membrane. The magnitude of this increase (ΔCm) reflects the number of vesicles that has undergone exocytosis. We used perforated whole-cell re-cordings to measure I_{Ca} and ΔCm evoked by two 100-ms steps from −80 to +10 mV (Fig. 7A) in chromaffin cells isolated from wild type mice. As already noted, cells could be separated into two groups based on the response of I_{Ca} to the application of PGE_2. In this particular series of experiments, PGE_2 (100 nM) inhibited the peak amplitude of I_{Ca} in 7 of 12 cells (group 1) by 41 ± 10% ($n = 7$; $p < 0.005$) but had no effect in the remaining 5 cells (group 2) (3 ± 4% decrease; $n = 5$; $p = 0.41$) (Fig. 7B). Application of 100 nM PGE_2 signifi-cantly reduced ΔCm in group 1 (those cells in which I_{Ca} was

Fig. 6. The inhibition of I_{Ca} produced by PGE_2 was abolished in cells isolated from EP3 receptor knockout mice. A, experimental time course plotting peak amplitude of I_{Ca} versus time from a representative cell isolated from an EP3 receptor knockout mouse [EP3(−/−) cells]. I_{Ca} was recorded in the conventional whole-cell configuration and elicited every 10 s with a 20-ms step depolarization from −80 to +20 mV. The cell was exposed first to 100 nM PGE_2 and subsequently to 100 μM ATP (to activate P2Y receptors), as indicated by the horizontal bars. PGE_2 had no effect on I_{Ca} recorded from EP3(−/−) chromaffin cells, whereas the inhi-bition produced by P2Y receptors remained intact. The inset shows three superimposed currents recorded before application of PGE_2 (ctl) during application of PGE_2 and during application of ATP. B, bar chart plotting the effects of PGE_2 and ATP on the mean peak amplitude of I_{Ca} in EP3(−/−) chromaffin cells (∗, $p < 0.05$; $n = 6$). C, data obtained from wild-type and EP receptor knockout mice using perforated whole-cell recording. Left, mean percentage of inhibition of I_{Ca} produced by PGE_2 in cells isolated from wild-type (wt) ($n = 15$) versus EP3 receptor knockout mice (EP3(−/−) ($n = 6$) (∗∗∗, $p < 0.001$). Right, percentage of inhibition of I_{Ca} produced by sulprostone (an EP1/EP3 selective agonist) in cells isolated from wild-type mice (wt) ($n = 6$) versus EP1 receptor knockout mice (EP1(−/−) ($n = 4$). (Wild-type data are from the same cells shown in Fig. 5B.).
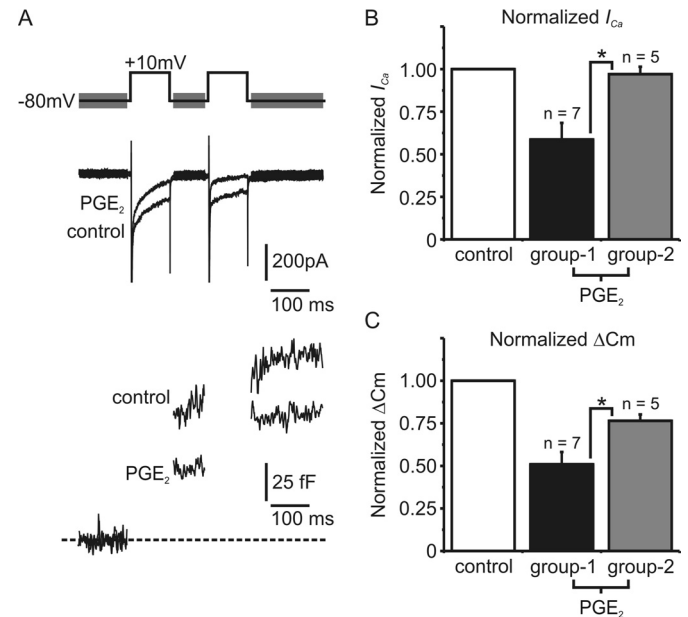

Fig. 7. Parallel inhibition of I_{Ca} and Ca^{2+}-dependent exocytosis by PGE_2. Perforated whole-cell recording was used to measure I_{Ca} and Cm in chromaffin cells isolated from wild-type mice. A, voltage command (top), I_{Ca} (middle), and membrane capacitance (bottom) recorded from a repre-sentative cell. Two superimposed recordings are shown in the absence (control) and presence of 100 nM PGE_2. The stimulus (top) consisted of two step-depolarizations (100-ms duration) from −80 to +10 mV. A 1-kHz sine wave was superimposed on the holding potential to calculate mem-brane capacitance (see *Materials and Methods* for details) and this was interrupted during the step-depolarizations as indicated. B, peak ampli-tude of I_{Ca} in the presence of PGE_2 was normalized to control I_{Ca} ampli-tude in the same cell (□, control). Cells were separated into two groups based on the response of I_{Ca} to application of PGE_2: group 1 (■; $n = 7$ of 12 cells), in which PGE_2 significantly reduced the amplitude of I_{Ca}, and group 2 (▨; $n = 5$ of 12 cells), in which PGE_2 did not inhibit I_{Ca} (∗, $p < 0.05$ comparing group 1 and group 2 in the presence of PGE_2). C, the change in membrane capacitance (ΔCm) in response to stimulation in the pres-ence of PGE_2 was normalized to ΔCm in control conditions in the same cell. ■, (group 1) data from cells in which I_{Ca} was inhibited (7 of 12 cells), and the ▨ (group 2) show data from cells in which I_{Ca} was not inhibited. ΔCm was reduced in both groups but the inhibition was significantly greater in group 1 compared with group 2 (∗, $p < 0.05$) (i.e., in those cells in which I_{Ca} was also reduced).

inhibited) from 153 ± 40 fF to 68 ± 16 fF ($n = 7$, $p < 0.03$). ΔCm was also significantly smaller during application of PGE$_2$ in group 2, even though I$_{Ca}$ was not reduced in these cells (Fig. 7C). This might reflect other pathways recruited by PGE$_2$ to control exocytosis independent of I$_{Ca}$ and/or time-dependent rundown of the exocytotic response, but these possibilities will require further investigation. It is noteworthy that the inhibition of ΔCm was significantly greater in group 1 cells (in which I$_{Ca}$ was also reduced) compared with group 2 cells ($49 \pm 7\%$, $n = 7$ compared with $24 \pm 4\%$, $n = 5$; $p < 0.02$) (Fig. 7C), consistent with the idea that inhibition of Ca^{2+} entry by PGE$_2$ leads to a parallel inhibition exocytosis as reported for other G$_{i/o}$-coupled GPCRs (Harkins and Fox, 2000; Powell et al., 2000; Ulate et al., 2000).

Discussion

Previous work has suggested that PGE$_2$ might modulate adrenal chromaffin cells, although the effects and EP receptors involved remained unclear. The synthetic enzymes for PGE$_2$ are present in the adrenal medulla, and cholinergic stimulation leads to release of prostaglandins from the intact adrenal gland (Ramwell et al., 1966). Furthermore, an in vivo analysis showed that systemic immune challenge or circulating cytokines rapidly recruited dendritic cells and macrophages to the adrenal gland and increased the expression of COX-2 and PGE synthase (Engström et al., 2008). Thus, periods of inflammation or stress might boost the production of PGE$_2$ within the adrenal gland. We reported previously that PGE$_2$ inhibited I$_{Ca}$ in bovine chromaffin cells, although the receptor(s) and detailed mechanisms were not determined (Currie et al., 2000). In contrast, others reported that PGE$_2$ stimulated calcium influx (Mochizuki-Oda et al., 1991) or released calcium from a ryanodine-sensitive intracellular store, an effect attributed to EP1 receptors (Shibuya et al., 1999). It has also been reported that PGE$_2$ inhibited nicotinic ACh receptors in sympathetic neurons (Tan et al., 1998). To our knowledge, this has not been tested in chromaffin cells, but if it were to occur, it could reduce cholinergic excitation/membrane depolarization and thereby opening of voltage-gated calcium channels.

In the current article, we report that PGE$_2$ inhibited I$_{Ca}$ in mouse chromaffin cells through pertussis toxin-sensitive G proteins. The inhibition was voltage-dependent (reversed by strong membrane depolarization) and preferentially targeted Ca$_V$2 calcium channels (N- and P/Q-type channels). Thus, PGE$_2$ mimicked agonists of other G$_{i/o}$-coupled GPCRs, including P2Y receptors that inhibit I$_{Ca}$ in chromaffin cells (Albillos et al., 1996; Currie and Fox, 1996; Powell et al., 2000). The inhibition by PGE$_2$ bore all of the hallmarks of that mediated by G$\beta\gamma$ subunit binding to the calcium channels (Currie, 2010a). To unequivocally identify the EP receptor subtype(s) involved, we used cells isolated from knockout mice that lack either the EP3 or EP1 receptors. To complement this genetic approach, we used selective pharmacological tools, including a recently described EP3 receptor antagonist, DG-041 (Heptinstall et al., 2008). Because this compound was not readily available, it was made in the Vanderbilt Institute for Chemical Biology Chemical Synthesis Core. Our data provide conclusive evidence that EP3 receptors mediated the inhibition of I$_{Ca}$ by PGE$_2$ in chromaffin cells.

It should be noted that PGE$_2$ inhibited I$_{Ca}$ in approximately three quarters of cells tested, presumably reflecting the expression of the EP3 receptor in this subpopulation of cells. In the rodent adrenal medulla 70 to 80% of chromaffin cells express phenylethanolamine *N*-methyltransferase, the enzyme that converts norepinephrine to epinephrine, so are termed "adrenergic" (Verhofstad et al., 1985). The remainder lack phenylethanolamine *N*-methyltransferase and are termed "noradrenergic." There is evidence for differential expression of GPCRs in adrenergic versus noradrenergic cells (Renshaw et al., 2000), so it is interesting to speculate that EP3 receptor expression might be limited to the adrenergic cells and preferentially modulate epinephrine release. Further work is required to determine whether this is the case. It is also noteworthy that the EP3 receptor undergoes alternative splicing, leading to sequence diversity in the cytoplasmic C terminus (Breyer et al., 2001). In recombinant systems, all of the splice variants couple to G$_{i/o}$-type G proteins but can also couple differentially to other effectors, including G$_s$, and G$_{12}$-RhoA. Because extracellular ligand binding is not altered, pharmacological distinction of the EP3 splice variants is not possible. Four alternatively spliced variants of the EP3 receptor have been identified in a bovine chromaffin cell library (Namba et al., 1993), and we detected mRNA for all three murine splice variants (EP3α, EP3β, and EP3γ) in the adrenal gland using RT-PCR (Fig. 4). However, a more detailed molecular analysis will be required to determine which splice variants are expressed in chromaffin cells and if additional non–G$_{i/o}$-coupled signaling pathways are recruited.

In contrast to some previous reports (Mochizuki-Oda et al., 1991; Shibuya et al., 1999), we found no evidence that PGE$_2$ can directly elevate [Ca^{2+}]$_i$ (Fig. 3C). PGE$_2$ had no effect on the holding current needed to voltage-clamp cells at -80 mV (i.e., did not open/close any channels) (Fig. 3A) and had no effect on resting [Ca^{2+}]$_i$ in Fura-2-loaded cells (Fig. 3C). It is possible that there are species differences in the expression of EP receptor subtypes because none of the previous studies used mice. We also found that PGE$_2$ had no effect on the peak amplitude of whole-cell nicotinic ACh receptor currents evoked by bath application of carbachol for 45 s (Fig. 3, A and B). However, we did note that there was a modest increase in current decay during the sustained application of carbachol in the presence of PGE$_2$ ($21 \pm 3\%$; $p < 0.01$ compared with $9 \pm 2\%$). Although "nondesensitizing" $\alpha3\beta4^*$-containing channels predominate in chromaffin cells, several other nicotinic receptor subunits are expressed in a species-dependent manner, including the rapidly desensitizing $\alpha7$ subunit (López et al., 1998; Sala et al., 2008). In chick sympathetic neurons, PGE$_2$ inhibited the whole-cell nicotinic current, but closer analysis revealed opposing effects on different channel subtypes. In particular, the dominant 36-pS channel was inhibited, but a 23-pS channel probably mediated by $\alpha7$ containing receptors was potentiated by PGE$_2$ (Du and Role, 2001). Further studies using fast, brief agonist applications are needed to fully address the effects of PGE$_2$ on nicotinic receptors, but our data do suggest that the predominant nondesensitizing nAChR current ($\alpha3\beta4^*$ receptors) is probably not a major target for PGE$_2$ modulation of chromaffin cell function.

Previous studies investigating the effects of PGE$_2$ on catecholamine secretion have all used large populations of cul-

tured chromaffin cells or intact adrenal gland preparations and present somewhat inconclusive findings. In some cases, PGE_2 inhibited release (Karaplis et al., 1989), whereas others report that PGE_2 potentiated release (Marley et al., 1988; Yamada et al., 1988; Yokohama et al., 1988). As discussed above, high concentrations of PGE_2 used in some of these studies raise the possibility of non-EP receptor involvement. Our data demonstrate for the first time that EP3 receptors use the same mechanism as P2Y, $\alpha2$-adrenergic, and μ-opioid receptors to inhibit voltage-gated calcium channels in chromaffin cells. Typically, such inhibition of I_{Ca} by GPCRs is paralleled by an inhibition of Ca^{2+}-dependent exocytosis, the mechanism that underlies vesicular catecholamine release (Harkins and Fox, 2000; Powell et al., 2000; Ulate et al., 2000). Exocytosis can be monitored in individual cells by tracking changes in membrane capacitance (ΔCm) that precisely reflect the surface area of a cell. The magnitude of ΔCm reflects the number of vesicles that have undergone exocytosis. As reported previously for other GPCRs, the application of PGE_2 led to a robust inhibition of ΔCm ($49 \pm 7\%$) that paralleled inhibition of I_{Ca} ($41 \pm 10\%$) (Fig. 7). There was also a modest decrease in ΔCm ($24 \pm 4\%$) in cells that showed no inhibition of I_{Ca}. This might reflect a time-dependent rundown of the exocytotic response or the possibility that other mechanisms are recruited to control secretion. $G\beta\gamma$-mediated inhibition of catecholamine release independent from I_{Ca} modulation has been reported for other $G_{i/o}$-coupled receptors (Chen et al., 2005; Yoon et al., 2008). We also detected mRNA for EP1, 2, and 4 receptors in the mouse adrenal gland, in addition to all three splice variants of the EP3 receptor (Fig. 4). Further detailed investigations will be required to determine whether these receptors are expressed in chromaffin cells and what functional affect they might have. However, our data clearly show that the inhibition of ΔCm was significantly greater when I_{Ca} was also reduced ($49 \pm 7\%$, $n = 7$ compared with $24 \pm 4\%$, $n = 5$; $p < 0.02$) (Fig. 7C), supporting the idea that inhibition of Ca^{2+} entry by PGE_2 leads to a parallel inhibition exocytosis as reported for other $G_{i/o}$-coupled GPCRs (Harkins and Fox, 2000; Powell et al., 2000; Ulate et al., 2000).

To summarize, there is growing interest in developing subtype-selective EP receptor drugs as therapeutic agents for a variety of disorders, so identifying the physiological roles distinct receptors play will be important for interpreting and predicting the affect of these drugs. We have used a powerful combination of pharmacology and cells isolated from receptor knockout mice to demonstrate that prostaglandin EP3 receptors inhibit I_{Ca} in adrenal chromaffin cells and that this results in a parallel inhibition of Ca^{2+}-dependent exocytosis. To our knowledge, this is the first study of EP receptor signaling in mouse chromaffin cells and identifies a cellular/molecular mechanism for paracrine regulation of neuroendocrine function by PGE_2.

Authorship Contributions

Participated in research design: Jewell, Breyer, and Currie.
Conducted experiments: Jewell.
Contributed new reagents or analytic tools: Breyer.
Performed data analysis: Jewell and Currie.
Wrote or contributed to the writing of the manuscript: Jewell, Breyer, and Currie.
Other: Breyer and Currie acquired funding for the research.

References

Albillos A, Carbone E, Gandía L, García AG, and Pollo A (1996) Opioid inhibition of Ca^{2+} channel subtypes in bovine chromaffin cells: selectivity of action and voltage-dependence. *Eur J Neurosci* **8:**1561–1570.

Boarder MR, Marriott D, and Adams M (1987) Stimulus secretion coupling in cultured chromaffin cells. Dependency on external sodium and on dihydropyridine-sensitive calcium channels. *Biochem Pharmacol* **36:**163–167.

Breyer MD, Jacobson HR, Davis LS, and Breyer RM (1993) In situ hybridization and localization of mRNA for the rabbit prostaglandin EP3 receptor. *Kidney Int* **44:**1372–1378.

Breyer RM, Bagdassarian CK, Myers SA, and Breyer MD (2001) Prostanoid receptors: subtypes and signaling. *Annu Rev Pharmacol Toxicol* **41:**661–690.

Chen XK, Wang LC, Zhou Y, Cai Q, Prakriya M, Duan KL, Sheng ZH, Lingle C, and Zhou Z (2005) Activation of GPCRs modulates quantal size in chromaffin cells through G(betagamma) and PKC. *Nat Neurosci* **8:**1160–1168.

Currie KP (2010a) G protein modulation of CaV2 voltage-gated calcium channels. *Channels* **4:**497–509.

Currie KP (2010b) Inhibition of Ca^{2+} channels and adrenal catecholamine release by G protein coupled receptors. *Cell Mol Neurobiol* **30:**1201–1208.

Currie KP and Fox AP (1996) ATP serves as a negative feedback inhibitor of voltage-gated Ca^{2+} channel currents in cultured bovine adrenal chromaffin cells. *Neuron* **16:**1027–1036.

Currie KP, Zhou Z, and Fox AP (2000) Evidence for paracrine signaling between macrophages and bovine adrenal chromaffin cell $Ca^{(2+)}$ channels. *J Neurophysiol* **83:**280–287.

Du C and Role LW (2001) Differential modulation of nicotinic acetylcholine receptor subtypes and synaptic transmission in chick sympathetic ganglia by PGE(2). *J Neurophysiol* **85:**2498–2508.

Dzhura EV, He W, and Currie KP (2006) Linopirdine modulates calcium signaling and stimulus-secretion coupling in adrenal chromaffin cells by targeting M-type K^+ channels and nicotinic acetylcholine receptors. *J Pharmacol Exp Ther* **316:**1165–1174.

Engström L, Rosén K, Angel A, Fyrberg A, Mackerlova L, Konsman JP, Engblom D, and Blomqvist A (2008) Systemic immune challenge activates an intrinsically regulated local inflammatory circuit in the adrenal gland. *Endocrinology* **149:**1436–1450.

García AG, García-De-Diego AM, Gandía L, Borges R, and García-Sancho J (2006) Calcium signaling and exocytosis in adrenal chromaffin cells. *Physiol Rev* **86:**1093–1131.

Guan Y, Zhang Y, Wu J, Qi Z, Yang G, Dou D, Gao Y, Chen L, Zhang X, Davis LS, et al. (2007) Antihypertensive effects of selective prostaglandin E2 receptor subtype 1 targeting. *J Clin Invest* **117:**2496–2505.

Harkins AB and Fox AP (2000) Activation of purinergic receptors by ATP inhibits secretion in bovine adrenal chromaffin cells. *Brain Res* **885:**231–239.

Heptinstall S, Espinosa DI, Manolopoulos P, Glenn JR, White AE, Johnson A, Dovlatova N, Fox SC, May JA, Hermann D, et al. (2008) DG-041 inhibits the EP3 prostanoid receptor–a new target for inhibition of platelet function in atherothrombotic disease. *Platelets* **19:**605–613.

Ichitani Y, Holmberg K, Maunsbach AB, Haeggström JZ, Samuelsson B, De Witt D, and Hökfelt T (2001) Cyclooxygenase-1 and cyclooxygenase-2 expression in rat kidney and adrenal gland after stimulation with systemic lipopolysaccharide: in situ hybridization and immunocytochemical studies. *Cell Tissue Res* **303:**235–252.

Ikeda SR (1992) Prostaglandin modulation of Ca^{2+} channels in rat sympathetic neurones is mediated by guanine nucleotide binding proteins. *J Physiol* **458:**339–359.

Irie A, Sugimoto Y, Namba T, Harazono A, Honda A, Watabe A, Negishi M, Narumiya S, and Ichikawa A (1993) Third isoform of the prostaglandin-E-receptor EP3 subtype with different C-terminal tail coupling to both stimulation and inhibition of adenylate cyclase. *Eur J Biochem* **217:**313–318.

Ji R, Chou CL, Xu W, Chen XB, Woodward DF, and Regan JW (2010) EP1 prostanoid receptor coupling to G i/o up-regulates the expression of hypoxia-inducible factor-1 alpha through activation of a phosphoinositide-3 kinase signaling pathway. *Mol Pharmacol* **77:**1025–1036.

Karaplis AC, Funk CD, and Powell WS (1989) Binding of prostaglandin E2 to cultured bovine adrenal chromaffin cells and its effect on catecholamine secretion. *Biochim Biophys Acta* **1010:**369–376.

López MG, Montiel C, Herrero CJ, García-Palomero E, Mayorgas I, Hernández-Guijo JM, Villarroya M, Olivares R, Gandía L, McIntosh JM, et al. (1998) Unmasking the functions of the chromaffin cell alpha7 nicotinic receptor by using short pulses of acetylcholine and selective blockers. *Proc Natl Acad Sci USA* **95:**14184–14189.

Lymperopoulos A, Rengo G, Zincarelli C, Soltys S, and Koch WJ (2008) Modulation of adrenal catecholamine secretion by in vivo gene transfer and manipulation of G protein-coupled receptor kinase-2 activity. *Mol Ther* **16:**302–307.

Marley PD, Bunn SJ, and Livett BG (1988) Prostanoid responses of bovine adrenal medullary cells: lack of effect of opioids. *Eur J Pharmacol* **145:**173–181.

Mochizuki-Oda N, Mori K, Negishi M, and Ito S (1991) Prostaglandin E2 activates Ca^{2+} channels in bovine adrenal chromaffin cells. *J Neurochem* **56:**541–547.

Namba T, Sugimoto Y, Negishi M, Irie A, Ushikubi F, Kakizuka A, Ito S, Ichikawa A, and Narumiya S (1993) Alternative splicing of C-terminal tail of prostaglandin E receptor subtype EP3 determines G-protein specificity. *Nature* **365:**166–170.

Powell AD, Teschemacher AG, and Seward EP (2000) P2Y purinoceptors inhibit

exocytosis in adrenal chromaffin cells via modulation of voltage-operated calcium channels. *J Neurosci* **20:**606–616.

Ramwell PW, Shaw JE, Douglas WW, and Poisner AM (1966) Efflux of prostaglandin from adrenal glands stimulated with acetylcholine. *Nature* **210:**273–274.

Renshaw D, Thomson LM, Michael GJ, Carroll M, Kapas S, and Hinson JP (2000) Adrenomedullin receptor is found exclusively in noradrenaline-secreting cells of the rat adrenal medulla. *J Neurochem* **74:**1766–1772.

Sala F, Nistri A, and Criado M (2008) Nicotinic acetylcholine receptors of adrenal chromaffin cells. *Acta Physiologica* **192:**203–212.

Shibuya I, Tanaka K, Uezono Y, Ueta Y, Toyohira Y, Yanagihara N, Izumi F, and Yamashita H (1999) Prostaglandin E2 induces Ca^{2+} release from ryanodine/caffeine-sensitive stores in bovine adrenal medullary cells via EP1-like receptors. *J Neurochem* **73:**2167–2174.

Tan W, Du C, Siegelbaum SA, and Role LW (1998) Modulation of nicotinic AChR channels by prostaglandin E2 in chick sympathetic ganglion neurons. *J Neurophysiol* **79:**870–878.

Ulate G, Scott SR, González J, Gilabert JA, and Artalejo AR (2000) Extracellular ATP regulates exocytosis in inhibiting multiple Ca^{2+} channel types in bovine chromaffin cells. *Pflugers Arch* **439:**304–314.

Verhofstad AA, Coupland RE, Parker TR, and Goldstein M (1985) Immunohistochemical and biochemical study on the development of the noradrenaline- and adrenaline-storing cells of the adrenal medulla of the rat. *Cell Tissue Res* **242:**233–243.

Yamada S, Morita K, Dohi T, and Tsujimoto A (1988) A modulating role of prostaglandins in catecholamine release by perfused dog adrenal glands. *Eur J Pharmacol* **146:**27–34.

Yokohama H, Tanaka T, Ito S, Negishi M, Hayashi H, and Hayaishi O (1988) Prostaglandin E receptor enhancement of catecholamine release may be mediated by phosphoinositide metabolism in bovine adrenal chromaffin cells. *J Biol Chem* **263:**1119–1122.

Yoon EJ, Hamm HE, and Currie KP (2008) G protein betagamma subunits modulate the number and nature of exocytotic fusion events in adrenal chromaffin cells independent of calcium entry. *J Neurophysiol* **100:**2929–2939.

Address correspondence to: Dr. Kevin Currie, Vanderbilt University School of Medicine, T4202 Medical Center North, Nashville TN 37232-2520. E-mail: kevin.currie@vanderbilt.edu